Membrane Structural Abnormalities in the Stratum Corneum of the Autosomal Recessive Ichthyoses

Ruby Ghadially, Mary L. Williams, Sui Yuen E. Hou, and Peter M. Elias

Dermatology Service, Veterans Administration Medical Center, San Francisco; and Department of Dermatology, University of California School of Medicine, San Francisco, California, U.S.A.

Congenital ichthyosiform erythroderma (CIE) and classic lamellar ichthyosis (LI) are autosomal recessive disorders of cornification (DOC), distinguished previously by clinical, histologic, ultrastructural, and cell kinetic criteria. Whether there is further heterogeneity within the CIE group is uncertain. To address the issue of genetic heterogeneity, and to study the pathogenesis of these DOC, skin biopsies from eight CIE, three LI, and six normal subjects were assessed by electron microscopy, including ruthenium tetroxide post-fixation with optical diffraction, to visualize and quantitate intercellular membrane domains. We found abnormal lamellar bodies in CIE and distinctive alterations in intercellular lamellar bilayer architecture among patients with CIE and three patients with LI. Two biopsies from two patients at different sites demonstrated the consistency of these findings. Moreover, in both CIE and the three LI patients, desmosomes persisted throughout the outer layers of the SC, indicative of impaired degradation. Our ultrastructural observations support the previously reported phenotypic distinction between CIE and LI, and the further likelihood of genetic heterogeneity within CIE. However, these studies do not support the division of the autosomal recessive ichthyoses into three subgroups based upon cytosolic structural abnormalities. Finally, these studies provide new insights into the pathogenesis of the autosomal recessive DOC. *J Invest Dermatol 99:755–763, 1992*

Mammalian stratum corneum comprises a two-compartment system of lipid-depleted corneocytes embedded in a lipid-enriched intercellular matrix (reviewed in [1]). These intercellular lipids are organized into a series of broad lamellar bilayers that regulate permeability barrier function and participate in the cohesion and desquamation of the stratum corneum (reviewed in [2]). Until recently, the intercellular membrane bilayer system could only be visualized reliably in freeze-fracture replicas [3–5]. With the recent advent of ruthenium tetroxide (RuO_4) post-fixation it is now possible to obtain ultrastructural images of the stratum corneum interstices on a routine basis [6,7], and a detailed tableau is emerging of the intercellular lamellar bilayer system in normal stratum corneum [1]. Moreover, this method already has been used to delineate the membrane structural basis for abnormal barrier function in murine essential fatty acid deficiency [7].

In normal stratum corneum, poorly understood changes occur in the stratum corneum interstices that lead to the orderly detachment of individual corneocytes at the skin surface. Alterations in lipid composition [8], the physical-chemical state of the lamellar bilayers [9], and/or degradation of non-lipid constituents such as desmosomes [10] all have been implicated as mediators of normal desquamation. The extent to which one or more of these processes is responsible for the desquamation of the DOC is still now known [2,11]. To address this issue we have applied the RuO_4 method to two types of autosomal recessive DOC, congenital ichthyosiform erythroderma (CIE) and classic lamellar ichthyosis (LI). Whereas CIE is characterized by variable fine scale, variable erythroderma, and epidermal hyperplasia, LI displays a uniformly severe clinical phenotype, unrelenting course, and essentially normal cell kinetics [12–14]. Despite these distinguishing clinical features and other reported biochemical differences, considerable controversy surrounds the nosology of these disorders [12–18]. Anton-Lamprecht and others (reviewed in [17,18]) have described ultrastructural criteria for three subsets of patients with ichthyosis congenita, a term that includes both CIE and LI: type I, numerous intracellular lipid droplets within corneocytes; type II, crystalloid inclusions, postulated to represent cholesterol crystals in corneocytes; and type III, elongated membrane structures in corneocytes, as well as vesicular complexes and vesicular lamellar bodies in granular cells. Whereas our studies reveal consistent heterogeneity of membrane structures within subgroups of CIE versus LI patients, and abnormalities in lamellar bodies in CIE, the features that have distinguished three subsets of autosomal recessive ichthyosis in other studies [17–19] did not identify clinical subgroups of our patients.

Manuscript received February 20, 1992; accepted for publication July 16, 1992.

Reprint requests to: Dr. Peter M. Elias, Chief, Dermatology Service (190), V.A. Medical Center, 4150 Clement Street, San Francisco, California 94121.

Abbreviations:
CIE: congenital ichthyosiform erythroderma
DOC: disorders of cornification
LI: lamellar ichthyosis

MATERIALS AND METHODS

Tissue Samples After obtaining informed consent, 3-mm punch biopsies were taken from both patients and normal controls (back, with additional samples from two patients from a second site). These included six normal controls, eight patients with CIE, and three patients with LI. The diagnoses were established by clinical and histologic characteristics, as described previously [12].

Tissue Preparation for Electron Microscopy Biopsy samples were minced to ≤ 1 mm^3 pieces and fixed overnight (~ 16 h) at 4°C in 2% glutaraldehyde and 2% paraformaldehyde with 0.06% calcium chloride in 0.1 M sodium cacodylate buffer, pH 7.3. Specimens then were placed in 0.1 M sodium cacodylate buffer prior to further processing. Portions of each tissue sample were placed in

0022-202X/92/$05.00

0.2% RuO_4 (Polysciences, Warrington, PA) with 0.5% potassium ferrocyanide in 0.1 M sodium cacodylate, pH 7.4, at room temperature and in the dark for 0.5 h, whereas others were placed in 1% osmium tetroxide with potassium ferrocyanide (1.5%) in 0.1 M sodium cacodylate at room temperature in the dark for 1 h. After rinsing in buffer, tissue samples were dehydrated in a graded ethanol series, and subsequently embedded in a low-viscosity, Epoxy resin containing DER 736 and Epon 812 [20]. Thin sections were examined using a Zeiss 10A electron microscope operating at 60 kV, after staining with lead citrate and/or uranyl acetate. Lamellar body dimensions were measureed in random micrographs from four normal, four CIE, and two LI samples (9 total of 200 organelles in 16 section).

Optical Diffraction, Image Analysis, and Reconstruction Electron micrographs of intercellular bilayer structures in RuO_4-fixed sections were screened for well-ordered areas by optical diffraction using a helium neon laser source [21]. The best-ordered regions in the images of lamellar stacks on the electron micrographs were digitized with a Perkin-Elmer PDS microdensitometer, utilizing an aperture size of 20 × 20 nm or 30 × 30 nm and a respective step-size of 20 nm or 30 nm, corresponding to an actual spacing of 5–10 Å in the imaged specimen. The optical densities of selected areas were "floated" to an array size of 512 × 512, 256 × 256, 128 × 128 pixels and then Fourier-transformed on computer [21]. A one-dimensional, least-squares refined lattice and the associated unit cell dimension were derived from the positions of the reflections [7]. The amplitudes and phases for these reflections were extracted, as described [21]. Using these amplitudes and phases, a one-dimensional optical density profile (representing stain excluding mass in the specimens) was derived by Fourier transformation. These profiles then were inverted to match the printed image (representing stain-including mass). Prior studies have shown that the lamellar dimensions obtained with this method, as applied to RuO_4-fixed material, match measurements of comparable unfixed stratum corneum assessed by X-ray diffraction [7,22].

RESULTS

Ultrastructure of Normal Stratum Corneum

Membrane Structure and Organization: The lamellae within the intercellular domains of normal human stratum corneum exhibit a similar organization and substructure to previous descriptions of porcine [6] and murine [7] stratum corneum. In optimal cross sections, these membranes can be seen to comprise three types of electron-lucent lamellae that alternate with a single type of electron-dense lamella (Fig 1). From the corneocyte envelope outward, the electron-lucent lamellae comprise, first, a continuous sheet immediately exterior to the cornified envelope [6,7,23]. The succeeding lamellae are organized external to adjacent lamellae with the center of the interrupted, lucent lamellae serving as the plane of symmetry. Each series of four electron-lucent lamellae alternating with five electron-dense lamellae, comprises the basic unit [7] (Fig 1, *inset*). At many points in the interstices this basic unit expands incrementally and suddenly, by the addition of arrays of continuous electron-dense and -lucent lamellae. A double basic unit (or "doublet") comprises two basic units minus one interrupted, electron-lucent lamella and two electron-dense lamellae, which result from sharing of these structures by two adjacent basic units (Fig 1, *bars*). Triple basic units ("triplets"), the largest units observed in normal human stratum corneum, also occur occasionally.

Corneocyte Interior in Normal Stratum Corneum: Examination of normal human corneocytes with RuO_4 showed a regular keratin pattern (Table I). Longitudinal membrane structures were encountered infrequently in five of the six normal controls (Fig 2*A*). Vesicular complexes were seen in two controls, but only infrequently (Fig 2C1).

Lamellar Body Structure in Normal Epidermis: Staining of lamellar bodies in the stratum granulosum with standard osmium tetroxide fixation provides excellent preservation of lamellar body structure.

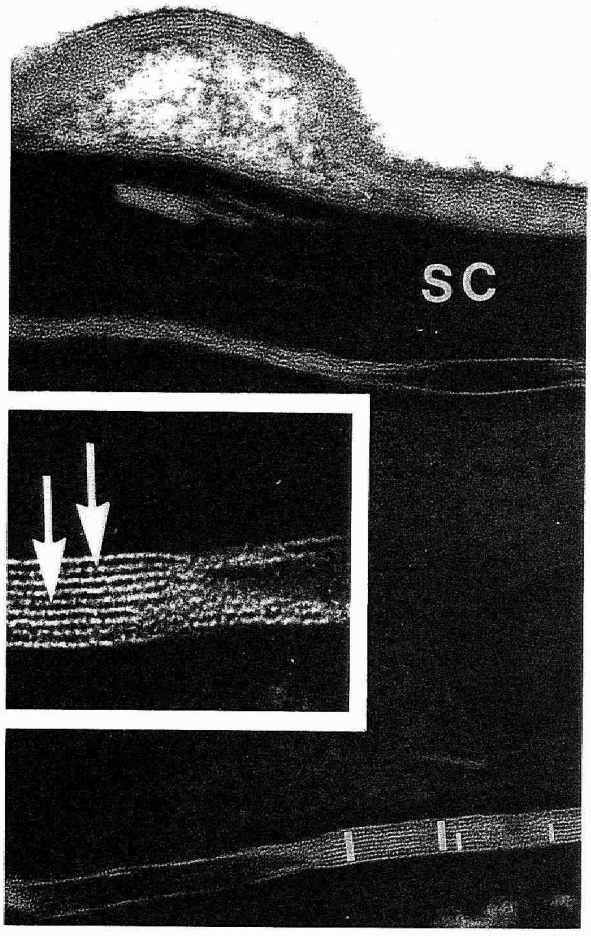

Figure 1. Normal human stratum corneum. Intercellular domains show presence of intercellular bilayer structures, with repeat pattern of lucent and dense bands (also see Fig 5*A*). *Inset,* high-power view of same. *Narrow bars,* single basic unit structure; *wider bars,* "doublet" (see text). Ruthenium tetroxide (RuO_4). Magnification × 155,000; inset, × 370,000.

Briefly, cross sectional images of lamellar bodies in normal epidermis demonstrated a trilaminar limiting membrane, and internal lamellar disc-like structures, consisting of prominent dense lamellae, separated by an electron-lucent hand, and divided centrally by a minor, striated electron-dense band (Fig 2*C*, *inset*).

Epidermal Ultrastructure in Congenital Ichthyosiform Erythroderma

Membrane Structure and Intercellular Organization (Table II): Whereas normal stratum corneum displayed the distinctive organization of lamellar bilayers shown in Fig 1, multiple abnormalities were seen in the intercellular domains of patients with CIE (Table II). The most striking findings, present in all or most of the CIE cases, were 1) foci containing excessive numbers of lamellae in stacks (Figs 3 and 4; cf, Fig 5); 2) a predominance of incompletely formed and/or disorganized lamellar arrays (Fig 4); 3) shortened arrays of lamellar body–derived membranes (Fig 4, *inset*); 4) variations in the substructure of individual lamellae, both within the lucent and dense bands (Fig 3*B*, *C*), and with abnormal interlamellar dimensions (see below for quantitative data); 5) electron-lucent domains, presumably representing non-lamellar phases because of the presence of

Table I. Changes in the Cytosol of the Stratum Granulosum and Stratum Corneum[a]

		CIE										LI		
	Normal (n = 6)	1A	1B	2	3	4	5A	5B	6	7	8	1	2	3
Lamellar bodies (LB)														
Increased numbers	−	+	+	+	+	+	NE	NE	+	+	+	−	−	NE
Decreased size	−	+	+	+	+	+	NE	NE	+	+	+	−	−	NE
Abnormal contents	−	+	+	+	+	+	NE	NE	+	+	+	−	−	NE
Lipid vacuoles														
In the stratum corneum	−	R	R	R	+	R	+	+	+	R	+	R	R	R
In the stratum granulosum	−	−	−	−	−	−	−	NE	−	−	−	−	−	NE
Longitudinal membrane structures														
In the stratum corneum	R	+	+	−	−	+	+	+	−	+	+	+	+	+
In the stratum granulosum	−	−	−	−	−	−	−	NE	−	−	−	−	−	NE
Crystalloid inclusions														
In the stratum corneum	−	−	−	−	−	−	+	−	−	−	−	−	−	−
In the stratum granulosum	−	−	−	−	−	−	−	NE	−	−	−	−	−	NE
Vesicular complexes														
In the stratum corneum	R	−	+	+	+	−	−	+	+	+	−	−	−	−
In the stratum granulosom	−	+	−	+	−	+	−	NE	+	−	−	−	−	NE

[a] NE, not examined; +, present; −, absent; A, B, different biopsies from same individual; R, rare.

flocculent, amorphous material (Fig 4) (such domains occurred interspersed between stacks of lamellar bilayers); and 6) finally, desmosomes, which normally deteriorate above the first six to eight layers of normal stratum corneum (Fig 6*A*), persisted in abundance in all of the 25-plus layers of the stratum corneum in CIE (Fig 6*B*).

In addition, the following features were seen in some, but not all patients (Table II) 1) Absence of the interrupted, electron-lucent lamella (three of seven cases; Fig 3*C*). This finding was consistent in one patient from two biopsies taken from different skin sites and separated chronologically by six months. 2) Decreased density of, as well as abnormal spacing of, the interrupted lamella was observed in four of seven patients (Figs 3*B*, *C*). This finding also was consistent in two biopsies taken from one patient several months apart.

Corneocyte Interior in CIE Stratum Corneum (Table I): Biopsies from patients with CIE showed a normal keratin pattern within corneocytes. Whereas some patients displayed large numbers of intracellular lipid droplets, others showed a few. Elongated membrane structures occurred in six of eight cases (Fig 2*B*). Vesicular complexes were seen in the stratum corneum of six of the eight patients (Table I; ultrastructural data not shown). Although these structures occurred occasionally in normal epidermis, they appeared in far greater numbers in CIE. A single patient showed crystalloid inclusions as well as elongated membrane structures in the SC (Fig 2*D*). However, a subsequent biopsy from the same patient failed to demonstrate comparable crystalloid inclusions in multiple sections of multiple blocks.

Lamellar Body Structure (Table I): Increased numbers of lamellar bodies were observed in the stratum granulosum in all CIE patients. Moreover, individual lamellar bodies appeared smaller than those of normal skin (Fig 2*C*; cf, *inset*) (CIE, mean diameter 154 ± 7.12 SE [n = 4 patients, 135 lamellar bodies]; normals, 175 ± 6.18 SE [n = 4 patients, 67 lamellar bodies]; $p < 0.05$). The internal contents of lamellar bodies from CIE epidermis were distinctly abnormal: most of these organelles appeared empty or contained only fragments of lamellar structures (Fig 2*C*), creating a vacuolated appearance. Finally, vesicular complexes were seen in the stratum granulosum in three of eight of these patients (Fig 2*C*; *asterisk*).

Epidermal Ultrastructure in Classic Lamellar Ichthyosis (LI)

Intercellular Domains in LI: In contrast to CIE, increased numbers of lamellae in stacks did not occur in the intercellular domains in LI (Fig 5). Moreover, the numbers of intercellular lamellae often appeared to be decreased due to their separation by extensive, largely empty lacunae or clefts within the electron-dense lamellae of membrane stacks (Fig 5). Furthermore, the intercellular lamellae in LI also showed an abnormal banding pattern, with an absence of the interrupted lamella that is invariably present in normal human stratum corneum (cf, Fig 1), and usually present in CIE samples (cf, Fig 3*B*). This resulted in alternating lucent and dense bands that appeared to be evenly spaced (Fig 5, *inset*), an observation confirmed by computer transforms of optical diffraction (see below). Finally, as in CIE, large numbers of desmosomes persisted within the intercellular spaces, even within the outermost layers of the hyperkeratotic stratum corneum (Fig 6*C*).

Corneocyte Interior (Table I): As in CIE, the stratum corneum from patients with LI showed a regular keratin pattern. Although lipid vacuoles were present in corneocytes, they were relatively few in number (Fig 6*C*). Longitudinal membrane structures were seen in all three LI patients (Fig 6, *asterisk*). However, neither cholesterol crystals nor vesicular complexes were seen.

Lamellar Body Structure: In contrast to CIE, the numbers, size, and internal contents of lamellar bodies in LI appeared comparable to normal controls (data not shown).

Quantitation of Lamellar Dimensions in Normal, CIE, and LI Stratum Corneum The optical density profiles of normal human stratum corneum intercellular lamellae resembled those from hairless mouse stratum corneum, both in terms of lamellar spacing (Table III) and optical density profile (Fig 7*B*) (cf [7]). Both methods indicate that the lamellar repeat unit in both species comprises two membrane bilayers. The optical density profiles of CIE differed from those of normal human stratum corneum (Fig 7*A*, *C*). In one case (patient 1) (Fig 7*A*), the continuous dense band that is present in normal tissue (indicated by the single peak in the optical density profile, Fig 7*B*) was both diminished and interrupted (*dashed* peaks in Fig 7*A* and actual image in Fig 3*B*). In another case (patient 3), the dense bands adjacent to the interrupted lucent band were diminished (lower density of double peak, Fig 7*C*). In both cases, the lamellar spacing was decreased in comparison to normal (Table III). However, in some areas the spacings were comparable to normal (e.g., patient 5, Table III). Because only selected areas from each case are amenable to this method of analysis, a statistical comparison of each patient to normal was not possible. However, when the data from both normal samples (n = 4 areas) and CIE subjects (n = 6 areas) were pooled, the average lamellar spacing of normal versus CIE was significantly different (125 ± 8 Å versus 109 ± 8 Å, respectively) ($p = 0.02$, t test) (Table III).

The optical density profile in the LI subjects was totally different from both normal and CIE, because the basic unit organization was absent. As noted above (Fig 5), only a single type of dense band,

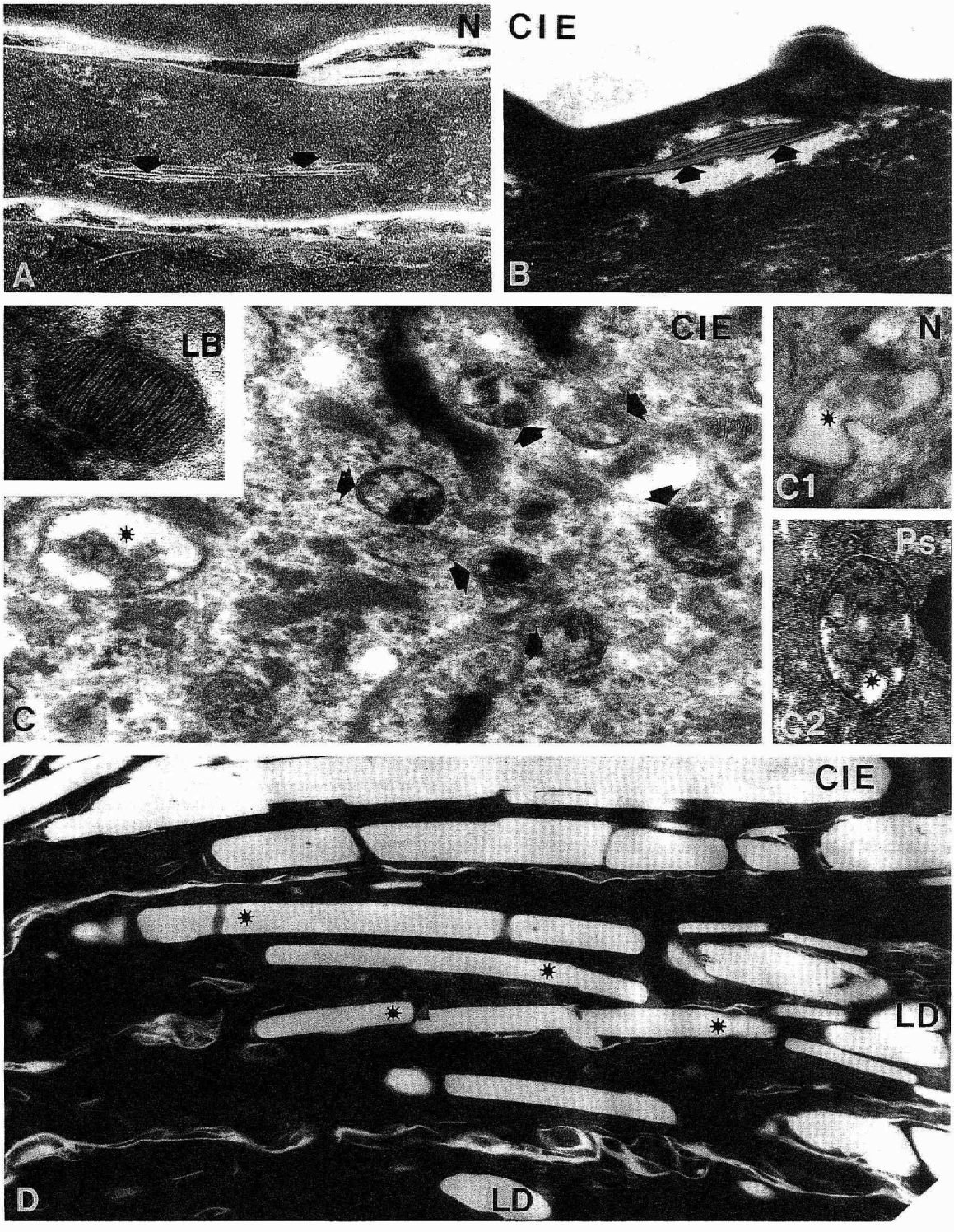

Figure 2. Comparison of cytosolic inclusions in CIE versus normal subjects. In *A* elongated membrane structures are seen in the corneocyte cytosol of normal stratum corneum *(arrows)*. *B* shows similar, elongated membranous structures in CIE *(arrows)*. Vesicular lamellar bodies *(arrows)* occur in the granular cell cytosol of all patients with CIE, but were not present in the three patients with LI (*C*; cf, normal lamellar body inset). *Inset*, normal lamellar body with disk-like, internal structures. However, vesicular complexes were seen not only in CIE *(asterisks)*, but also occasionally in normal skin *(C1, asterisk)*, and in psoriasis *(C2, asterisk)*. Crystalloid inclusions *(D, asterisks)* were seen in only one patient with CIE. Magnification: A (RuO_4, × 100,000; *B* (RuO_4), × 63,000; *C* (OsO_4), × 121,000; *inset* (RuO_4) × 168,000; *C1* (OsO_4), × 80,000; *C2* (RuO_4), × 112,500; *D* (RuO_4), × 29,500.

Table II. Membrane Abnormalities in the Stratum Corneum of Study Patients[a]

		CIE										LI		
Observations	Normal (n = 6)	1A	1B	2	3	4	5A	5B	6	7	8	1	2	3
Foci of increased numbers of lamellae	−	+	+	+	+	+	+	+	−	−	NE	−	−	−
Incompletely formed/disorganized lamellar arrays	−	+	+	+	+	+	+	+	+	+	NE	+	+	+
Shortened lamellar arrays	−	+	+	+	+	+	+	+	+	+	NE	+	+	+
Absence/abnormal density of interrupted lamellae	−	Abn	Abn	Abn	Abn	Abn	Abs	Abs	Abs	Abs	NE	Abs	Abs	Abs
Basic unit pattern (cf, Table III)	−	Abn	Abn	Abn	Abn	Abn	Abn	Abn	Abn	Abn	NE	Abs	Abs	Abs
Cleft formation ("phase separation")	−	+	+	+	+	+	+	+	+	+	NE	+	+	+
Persistent desmosomes	−	+	+	+	+	+	+	NE	+	+	+	+	+	+

[a] Abn, abnormal; Abs, absent; see Table I for explanations of other abbreviations.

alternating with a single type of lucent band, is present (peaks versus valleys in Fig 7*D*), and the interrupted lamella is absent. Therefore, the lamellar repeat distance, dense-band to dense-band spacing, and lucent-band to lucent-band separation was 29 Å in the one patient with a sample amenable to analysis (Table III).

DISCUSSION

Based upon clinical, histologic, cell kinetic, and lipid biochemical markers, the autosomal recessive forms of ichthyosis have been divided into two subgroups, CIE and LI [12–14]. Clinically, CIE displays a fine white scale pattern and a variable erythroderma. In mildly affected CIE patients, the erythroderma is less obvious, but generalized scaling involving the entire body surface serves to distinguish these patients from other milder DOC phenotypes, such as ichthyosis vulgaris or recessive X-linked ichthyosis [11,12]. In contrast, LI is characterized by thick, plate-like scales and a less intense erythroderma. Furthermore, LI is characterized by relatively normal cell proliferation kinetics, whereas CIE displays accelerated mitotic rates [13]. Finally, although a striking increase in the content of n-alkanes has been used to distinguish CIE from LI [12,14], recent ^{14}C-dating studies demonstrate an exogenous origin for these hydrocarbons [24,25].

We describe here the ultrastructural features of these two subgroups. Patients with CIE displayed abnormal lamellar bodies, often numerous lipid droplets within cornified cells, and extensive bilayer stacks within the intercellular spaces of the stratum corneum, features that were not seen in the three patients with LI. Moreover, a distinctive feature of both CIE and LI stratum corneum is the presence of non-lamellar domains interspersed between lamellae, forming clefts or large lacunae. These foci presumably represent regions where phase separation has occurred rather than artefactual separation within the intercellular spaces (cf, Fig 4), because they contain variable amounts of stainable amorphous material. Similar domains have been observed in two other, recessively inherited DOC associated with lipid abnormalities [26,27]. Such areas could result from the altered SC lipid composition present in these disorders, presumably because a proportion of the lipid in an "imbalanced" lipid mixture may not be completely integrated into a bilayer configura-

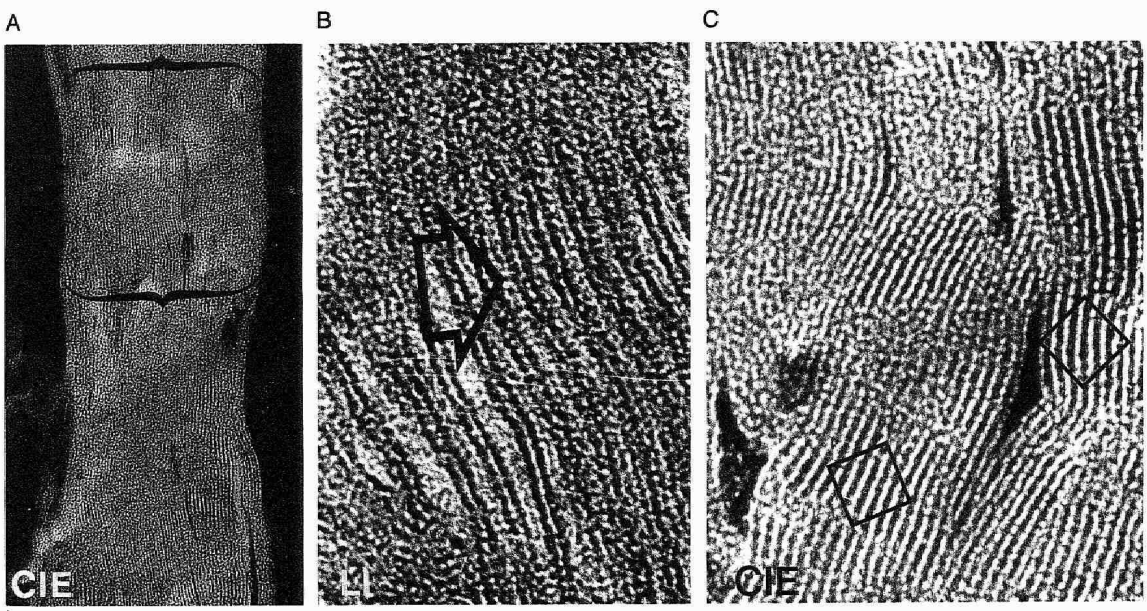

Figure 3. Stratum corneum from patients with CIE. Between corneocytes stained densely with ruthenium, note increased numbers of lamellae in stacks *(A, brackets)*. In some CIE patients, an abnormal or diminished interrupted lamellae is seen. Also, the interrupted bands are dense rather than lucent *(B, arrow)*, a reversal of the normal pattern. Another CIE phenotype shows a complete absence of interrupted lamellae within an expanded stack *(C, box)*. All RuO_4 fixed. Magnification: *A*, × 115,000; *B* × 700,000; *C*, × 650,000.

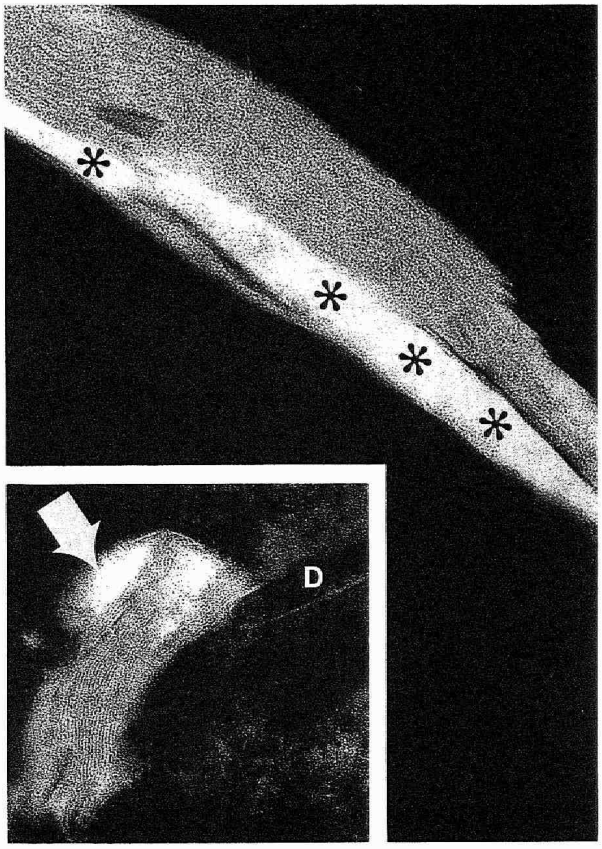

Figure 4. Stratum corneum from patients with CIE. Apparent phase separation of lipids into lamellar and nonlamellar domains *(asterisks)*, and disorganization and fragmentation of lamellar arrays as well as shortened lamellar arrays *(inset arrow)*. (All RuO_4 fixed.) Magnification: × 180,000; *inset* × 40,000.

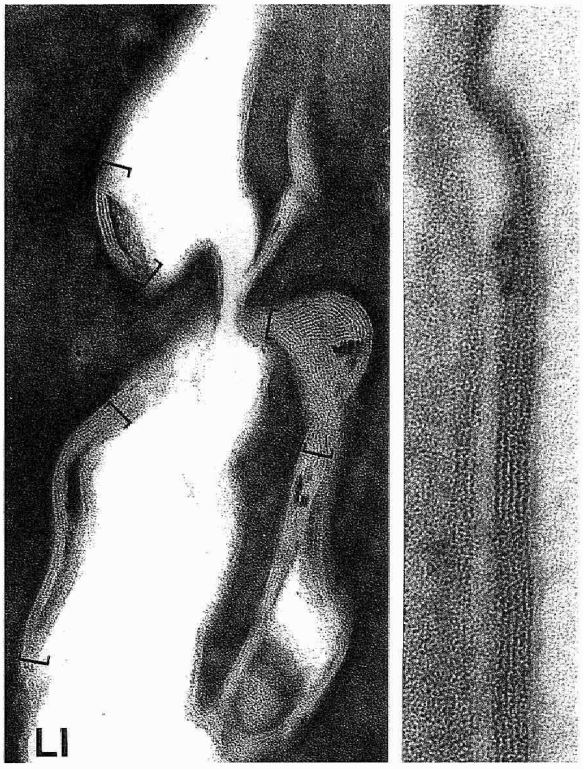

Figure 5. Stratum corneum from patients with LI. The numbers of intercellular lamellae appear decreased in number *(brackets)* due to separation artefacts and/or clefts within electron-dense lamellae. *Inset,* absence of an interrupted band, with even spacing of lucent and dense bands. All RuO_4 fixed. Magnification: × 93,000; *inset,* × 127,000.

tion; i.e., the excess (or non-integratable) lipids would form non-lamellar domains. Alternatively, these domains may result from permeation of exogenous lipid into the intercellular domains, as has recently been shown when petrolatum is added to the skin [25,28]. Although these studies also emphasize the desirability of obtaining biopsy sites free of exogenous lipids, it is often difficult to eliminate contamination with lipid-containing moisturizers. Despite these concerns, the wide-spread changes in these samples versus the focal nature of findings in moisturizer-treated samples [28], along with the consistency of findings in biopsies from the same patients at different dates and sites, further suggest that the phase separation in our samples is unlikely to be attributable to exogenous lipid applications.

In the European literature the term "ichthyosis congenita" often is used to refer to the group of disorders classified as autosomal recessive ichthyosis in North America. Whereas the autosomal recessive ichthyoses have been divided by some authors into CIE and LI (cited in [12], ichthyosis congenita has been divided into three types based upon electron-microscopic findings [17,18]. These include patients with 1) numerous intracellular droplets within corneocytes; 2) crystalloid inclusions, postulated to represent cholesterol crystals within corneocytes; and 3) elongated membranous inclusions within corneocytes, as well as vesicular lamellar bodies and vesicular complexes within granular cells. Our findings did not corroborate such subdivisions. First, longitudinal membrane structures were seen in the corneocytes of most normals, and in both CIE and LI. Furthermore, we have observed comparable membrane structures in psoriatic stratum corneum (Ghadially R, Elias PM, unpublished observations) and similar structures also have been reported in Sjögren-Larsson syndrome [29]. Thus, these structures appear to represent a normal variant that may represent incompletely degraded organelle membranes, which would be expected to occur more frequently in hyperproliferative dermatoses, such as CIE and psoriasis. Although vesicular complexes were seen only rarely in normals, they were encountered in all CIE samples, and also have been seen by us in psoriasis (Fig 2*C2*), as well as in mice treated topically with HMGCoA reductase inhibitors, such as lovastatin (Ghadially R, Menon GK, unpublished observations). These structures may represent lamellar bodies that do not mature in hyperproliferative states, such as CIE or psoriasis, or, alternatively, they could reflect altered epidermal lipogenesis, as occurs with lovastatin treatment [30]. Their absence in LI, a normoproliferative disorder [13], would be consistent with this hypothesis. Finally, crystalloid inclusions were seen in only a single patient with CIE (patient 5), and only in one of two biopsies from this subject. This patient had the clinical phenotype of severe CIE and exhibited all of the ultrastructural changes in stratum corneum membranes found in this disorder, as well as elongated cytosolic membrane structures (a feature of ichthyosis congenita, type III) and numerous vesicular structures (a feature of ichthyosis congenita, type I). Thus, longitudinal membrane structures appear to be a non-specific feature of both normal and ichthyotic stratum corneum, whereas vesicular complexes (and longitudinal membrane structures) may be linked to hyperproliferation, and although crystalloid inclusions may be an inconstant, and hence unreliable, diagnostic feature. Thus, in our

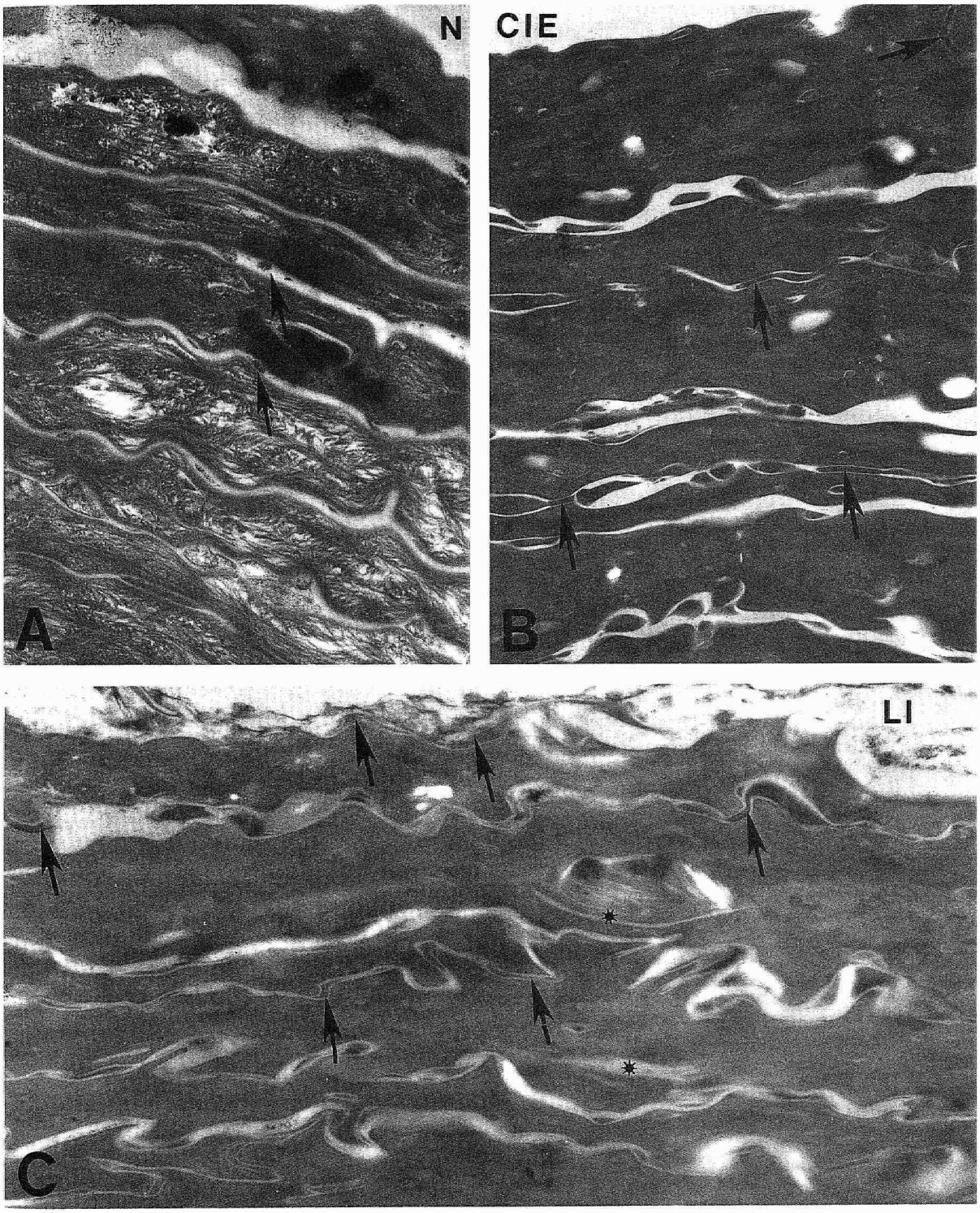

Figure 6. Desmosomes in subjects with normal, CIE, and LI stratum corneum (SC). In normal SC, the outermost SC layers demonstrate very few desmosomal remnants above the fifth cell layer *(A, arrows)*. Residual desmosomal structures are seen only at lower levels of the SC. Likewise, in the SC of CIE the outermost layers (20–25) display extensive numbers of desmosomal remnants *(B, arrows)*. In the SC of LI the outermost layers (20–25) show extensive desmosomal remnants *(arrows)*. All OsO_4 fixed. Magnification: *A*, × 41,000; *B*, × 43,000; *C*, × 41,000.

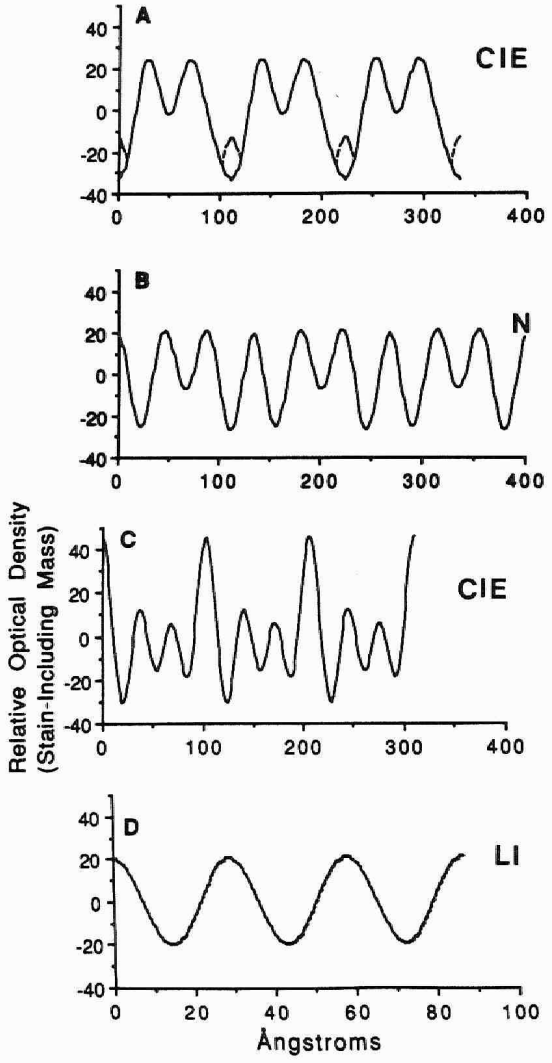

Figure 7. Reconstructed optical density profiles of stratum corneum lamellae: cross-sectional electron micrograph images. *A*) CIE: dashed peaks were drawn in, and not present in the reconstructed profile, presumably because of their irregularity. This profile corresponds to the image shown in Fig 5*B* (patient 1); *B*) normal human subject (patient 1); *C*) CIE (patient 3); *D*) LI (note that this is a cosine wave). Three repeat units are shown for each case. The optical densities (arbitrary scale for each profile) shown have been inverted from those after reconstruction to correspond to those in the printed image.

experience these ultrastructural features were not reliable or diagnostically useful markers of disease subsets.

Increased numbers of lamellar bodies have previously been reported in hyperproliferative disorders, such as psoriasis [31,32] and essential fatty acid deficiency (EFAD) [33]. We noted here an apparent increase in the numbers, along with a significant decrease in the size of lamellar bodies in all subjects with CIE, which is also a hyperproliferative disorder [13]. In contrast, the numbers of lamellar bodies did not appear to be increased in LI (a normoproliferative disorder). However, apparent changes in the quantities of LB need to be interpreted with caution because of the lability of these structures.

In contrast to lamellar body numbers, which may correlate with proliferation, desmosomal structures persisted well into the upper layers of the stratum corneum in both CIE and LI (i.e., more than 20–30 layers). Similar desmosomal retention also has been noted previously in two other DOC, recessive X-linked ichthyosis [34] and Refsum syndrome [35]. Menon et al [36] have suggested that desmosomal persistence may be due to defective delivery of lamellar body–derived hydrolytic enzymes to the intercellular spaces in some DOC, including CIE. Indeed, Bergers et al [15] recently have shown distinct differences in stratum corneum hydrolase profiles between erythrodermic and non-erythrodermic subsets of autosomal recessive lamellar ichthyosis, which could reflect differences in hydrolase packaging and/or delivery. One of us (MLW) has also proposed that alterations in stratum corneum lipid composition, as occurs in RXLI, also could alter hydrolase activity [2]. Thus, abnormal lamellar body hydrolase content and/or delivery or abnormalities in stratum corneum lipid composition and organization alone or in combination could result in abnormal desmosomal persistence [2]. Abnormal desmosomal persistence may be the final common pathway through which delayed desquamation occurs in a number of DOC.

The image-processing techniques used here, namely, computed transform and optical density reconstruction, allow electron micrographic images of the stratum corneum intercellular lamellae from various specimens to be compared quantitatively with respect to lamellar dimensions or spacings and semi-quantitatively with respect to image optical density (indicative of the structure of the lamellae normal to the plane of stratum corneum). The validity of the dimensions obtained with this method has been shown previously [7,21], where similar lamellar spacings were obtained by optical and X-ray diffraction in parallel tissue samples of diseased and normal stratum corneum. As we have suggested previously [7], the absence of shrinkage artefacts may be due to the lack of water within the hydrophobic bilayer structure of stratum corneum, because X-ray diffraction of hydrated versus dry samples gave similar lamellar spacings. This contrasts with observations on phospholipid-enriched biologic membranes that can be heavily hydrated, and are subject to extensive artefacts in association with biologic fixation [37]. Bilayer dimensions were compared in normal subjects versus those with both CIE and LI. Though the electron microscopic bilayer patterns of various CIE samples varied, optical diffraction studies suggested that bilayer narrowing is a relatively constant feature of CIE. In the one LI sample, the usual lamellar repeat unit organization was not seen. Repeat biopsies from selected patients performed both at later dates and from different skin sites confirm the reproducibility and reliability of the ruthenium tetroxide technique.

In summary, these studies demonstrate heterogeneity of stratum

Table III. Membrane Dimensions Obtained from Optical Diffraction and Computer Transforms of Study Samples

Disease	Patient	Lamellar Spacing (Å) Individual Areas	Mean
Normal human	1	136	
		120	125 ± 10
		118	
	2	126[a]	126
CIE	1	112	105
		98	
	3	113[a]	109
		104	
	5	122[a,b]	116
		109[a,b]	
LI	1	29	29
		28	

[a] These values represent three times the spacing corresponding to the third-order spot in the pattern. A direct determination of the lamellar spacing was not possible due to the limited size of the lamellar stacks in the areas examined as subsidiary spots arose.
[b] From optical diffraction.

corneum intercellular membrane architecture among patients within the CIE phenotype. These differences were preserved in two patients in whom subsequent biopsies were obtained, suggesting that they may represent consistent phenotypic differences. Whether these differences reflect underlying genotypic differences within the CIE group cannot be established from the present study, and will require further studies of CIE kindreds. The most distinct differences between CIE and LI were the presence of numerous lipid droplets within cornified cells, large numbers of small, defective lamellar bodies, and the presence of extensive membrane stacks with abnormal lamellar basic unit patterns and dimensions. Although these data support the hypothesis that CIE and LI represent different genotypes, the number of patients with LI in this study were too few to permit definitive conclusions. Finally, these studies reveal consistent abnormalities in membrane structure that it has previously not been possible to evaluate, due to the lack of methods for the visualization of the contents of the stratum corneum intercellular spaces. The RuO_4 methodology should yield new information about structural markers and pathogenic mechanisms in a variety of other scaling dermatoses.

This work was supported by National Institutes of Health grants AR 29908 and AR 19098, the Medical Research Service, Veterans Administration, the American Federation of Aging Research, and the Lester E. Conrad Foundation. Dr. Ghadially was a recipient of a Dermatology Foundation Fellowship. Noel E. Taylor (deceased) and Robyn Stierwalt provided excellent technical assistance; Bil Chapman and Raymond Pelayo capably prepared the manuscript.

REFERENCES

1. Elias PM, Menon GK: Structural and lipid biochemical correlates of the epidermal permeability barrier. Adv Lipid Res 24:1–23, 1991
2. Williams ML: Lipids in normal and pathological desquamation. Adv Lipid Res 24:211–298, 1991
3. Elias PM, Friend DS: The permeability barrier in mammalian epidermis. J Cell Biol 65:180–191, 1975
4. Elias PM, Goerke J, Friend D: Mammalian epidermal barrier layer lipids: composition and influence on structure. J Invest Dermatol 69:535–546, 1977
5. Elias PM, McNutt NS, Friend D: Membrane alterations during cornification of mammalian squamous epithelia: a freeze-fracture, tracer and thin-section study. Anat Rec 189:577–593, 1977
6. Swartzendruber DC, Wertz PW, Kitko DJ, Madison KC, Downing DT: Molecular models of the intercellular lipid lamellae in mammalian stratum corneum. J Invest Dermatol 92:251–257, 1989
7. Hou SYE, White SH, Menon GK, Grayson S, Ghadially R, Elias PM: Membrane structures in normal and essential fatty acid deficient stratum corneum: characterization by ruthenium tetroxide staining and x-ray diffraction. J Invest Dermatol 96:215–223, 1991
8. Lampe MA, Williams ML, Elias PM: Human epidermal lipids: characterization and modulations during differentiation. J Lipid Res 24:131–140, 1983
9. Rehfeld SJ, Plachy WZ, Williams ML, Elias PM: Calorimetric and electron spin resonance examination of lipid phase transitions in human stratum corneum: molecular basis for normal cohesion and abnormal desquamation in recessive X-linked ichthyosis. J Invest Dermatol 91:499–505, 1988
10. Egelrud T, Hofer P-A, Lundström A: Proteolytic degradation of desmo-somes in plantar stratum corneum leads to cell dissociation in vitro. Acta Derm Venereol (Stockh) 68:93–97, 1988
11. Williams ML, Elias PM: Genetically transmitted, generalized disorders of cornification: the ichthyoses. In: Alper JC (ed.). Dermatology Clinics of North America. WB Saunders Company, Philadelphia, 1987, pp 155–178
12. Williams ML, Elias PM: Heterogeneity in autosomal recessive ichthyosis: clinical and biochemical differentiation of lamellar ichthyosis and non-bullous congenital ichthyosiform erythroderma. Arch Dermatol 121:477–488, 1985
13. Hazell M, Marks R: Clinical, histologic, and cell kinetic discrimination between lamellar ichthyosis and non-bullous congenital ichthyosiform erythroderma. Arch Dermatol 121:489–493, 1985
14. Williams ML, Elias PM: Elevated n-alkanes in congenital ichthyosiform erythroderma: phenotypic differentiation of two types of autosomal recessive ichthyosis. J Clin Invest 74:296–300, 1984
15. Bergers M, Traupe H, Dunnwald SC, Mier PD, van Dooren-Greebe R, Steijilen P, Happle R: Enzymatic distinction between two subgroups of autosomal recessive lamellar ichthyosis. J Invest Dermatol 94:407–412, 1990
16. Bernhardt M, Baden HP: Report of a family with an unusual expression of recessive ichthyosis; review of 42 cases. Arch Dermatol 122:428–433, 1986
17. Arnold ML, Anton-Lamprecht I, Melz-Rothfuss B, Hartschuh W: Ichthyosis congenita type III. Arch Dermatol Res 280:268–278, 1988
18. Traupe H: The lamellar ichthyoses. In: Traupe H (ed.). The Ichthyoses. Springer-Verlag, New York, 1989, pp 111–134
19. Niemi K-M, Kanerva L, Kuokkamen K: Recessive ichthyosis congenita type II. Arch Dermatol Res 283:211–218, 1991
20. McNutt NS, Crain WL: Quantitative electron microscope comparison of lymphatic nuclear contours in mycosis fungoides and in benign infiltrates of the skin. Cancer 47:163–166, 1981
21. Ross MJ, Klymkowsky MW, Agard DA, Stroud RM: Structural studies of a membrane-bound acetylcholine receptor for Torpedo California. J Mol Biol 116:635–659, 1977
22. White SH, Mirejovsky D, King GI: Structure of lamellar lipid domains and corneocyte envelopes of murine stratum corneum. An X-ray diffraction study. Biochemistry 27:3725–3732, 1988
23. Swartzendruber DC, Wertz PW, Madison KC, Downing DT: Evidence that the corneocyte has a chemically bound lipid envelope. J Invest Dermatol 88:709–713, 1987
24. Bortz JT, Wertz PW, Downing DT: The origin of alkanes found in human skin surface lipids. J Invest Dermatol 93:723–727, 1989
25. Williams ML, Vogel JS, Ghadially R, Brown BE, Elias PM: Exogenous origin of n-alkanes in pathological scale. Arch Dermatol 128:1065–1071, 1992
26. Elias PM, Williams ML: Neutral lipid storage disease with ichthyosis: defective lamellar body contents and intercellular dispersion. Arch Dermatol 121:1000–1008, 1985
27. Koone MD, Rizzo WB, Elias PM, Williams ML, Lightner V, Pinnell SR: Ichthyosis, mental retardation, and asymptomatic spasticity: a new neurocutaneous syndrome with normal fatty alcohol:NAD^+ oxidoreductase activity. Arch Dermatol 126:1485–1490, 1990
28. Ghadially R, Elias PM, Halkier-Sorensen L: The effects of petrolatum on stratum corneum structure and function. J Am Acad Dermatol 26:387–396, 1992
29. Ito M, Oguro K, Sato Y: Ultrastructural study of the skin in Sjögren-Larsson syndrome. Arch Dermatol Res 283:141–148, 1991
30. Feingold KR, Mao-Qiang M, Proksch E, Menon GK, Brown B, Elias PM: The lovastatin-treated rodent: a new model of barrier disruption and epidermal hyperplasia. J Invest Dermatol 96:201–209, 1991
31. Mottaz JH, Zelickson AS: Keratinosomes in psoriatic skin. Acta Dermato Venereol (Stockholm) 55:81–85, 1975
32. Van de Staak WJBM, Stadhouders AM, Gilsing HMV: Keratinosomes in psoriatic skin. Acta Dermatovenereol 48:181–185, 1968
33. Elias PM, Brown BE: The mammalian cutaneous permeability barrier: defective barrier function in essential fatty acid deficiency correlates with abnormal intercellular lipid deposition. Lab Invest 39:574–583, 1978
34. Mesquitas-Guimaraes J: X-linked ichthyosis. Dermatologica 162: 157–166, 1981
35. Blanchet-Bardon CL, Anton-Lemprecht I, Puissant A, Schnyder A: Ultrastructural features of ichthyotic skin in Refsum's syndrome. The Ichthyoses (Marks R, Dykes PH (eds.). MTP Press, Lancaster, England 1977, pp 65–69
36. Menon GK, Ghadially R, Williams ML, Elias PM: Lamellar bodies as delivery systems of lipolytic enzymes: implications for corneocyte cohesion and desquamation. Br J Dermatol 126:337–345, 1992
37. Ghadially FN: Lysosomes. In: Ultrastructural Pathology of the Cell and Matrix, Chap. 7. Butterworths, London, 1988, p 620